Davod Poreh

Tutor: Daniele Riccio

XXX Cycle - II year presentation

Electromagnetic modeling for SAR polarimetry and interferometry

Motivations

- Synthetic Aperture Radar (SAR) images are essential tools for natural resource monitoring, environmental hazards, managements, control, etc.
- SAR data contain huge information about physical and chemical properties of the illuminated surface of the Earth.
- The main aim of my research activity is to model and use SAR and InSAR data, to retrieve and simulate ground surface information, that would be useful for many scientific disciplines. This is accomplished via my research archetype:
- Usage of SAR Polarimetry: SAR Polarimetry has been successfully modeled and applied to soil moisture retrieval in bare surface and/or for medium vegetated surfaces.
- Simulate SAR Polarimetry: Polarimetric SAR raw signal simulator, based on a sound physical electromagnetic scattering model, has been successfully modeled and applied for bare surfaces [1].
- Usage of SAR Interferomety: Space-borne Differential Interferometric Synthetic Aperture Radar (DInSAR) techniques and specifically Persistent Scatterer Interferometry (PSI) have shown their capabilities in monitoring of Earth surface displacements. We applied PSI methodology for monitoring of the earth surface changes and railways at the Campania region.

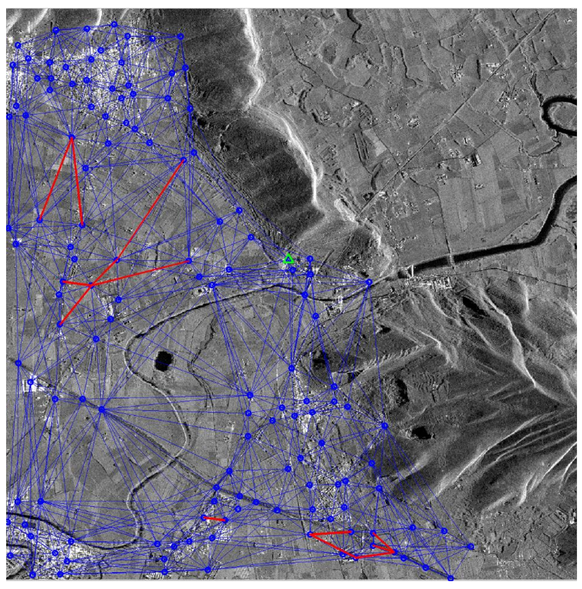

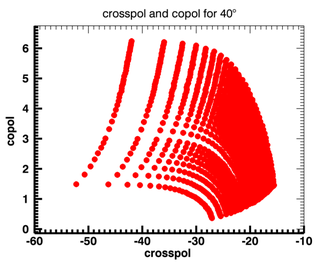

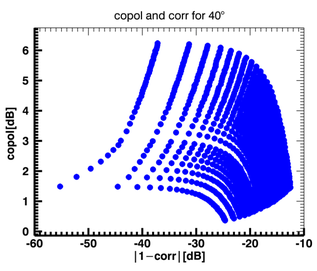

THEORETICAL FRAMEWORK:

SAR Polarimetry

Computation of reflectivity map in SARAS must be modified properly:

$$h(x',r') = \iint g(x'-x, r'-r; x, r)\gamma(x,r)dxdr$$

Zero-mean random deviations of the facets' azimuth and range slopes are added

$$p(\delta a, \delta b) = \frac{1}{\sqrt{2\pi}\sigma_x} e^{-\frac{\delta a^2}{2\sigma_x{}^2}} \cdot \frac{1}{\sqrt{2\pi}\sigma_y} e^{-\frac{\delta b^2}{2\sigma_y{}^2}}$$

Same realization of random variable in Small Perturbation Method (SPM) or the Physical Optics (PO) regimes, in such a way to guarantee that three polarimetreic channels are not independent. However, the facet slopes' randomness, ensures de-correlation among the three polarimetirc channels

$$\gamma_{pq}(x,r;\vartheta_l,\beta) = \chi_{pq}(x,r;\vartheta_l,\beta)w(x,r;\vartheta_l)$$

$$\underline{\underline{\chi}}_{pq}(\vartheta_l,\beta) = \underline{\underline{R}}_2(\beta)\begin{pmatrix} F_H(\vartheta_l) & 0 \\ 0 & F_V(\vartheta_l) \end{pmatrix}\underline{\underline{R}}_2{}^{-1}(\beta)$$

$$< |w(\vartheta_l)|^2 > = k^4 \cos^4\vartheta_l W(2k\sin\vartheta_l)$$

$$\begin{cases} copol = \dfrac{\langle |i_{HH}|^2 \rangle}{\langle |i_{VV}|^2 \rangle} \\ crosspol = \dfrac{\langle |i_{HV}|^2 \rangle}{\langle |i_{VV}|^2 \rangle} \\ corr = \dfrac{|\langle i_{HH} i_{VV}^* \rangle|}{\sqrt{\langle |i_{HH}|^2 \rangle \langle |i_{VV}|^2 \rangle}} \end{cases}$$

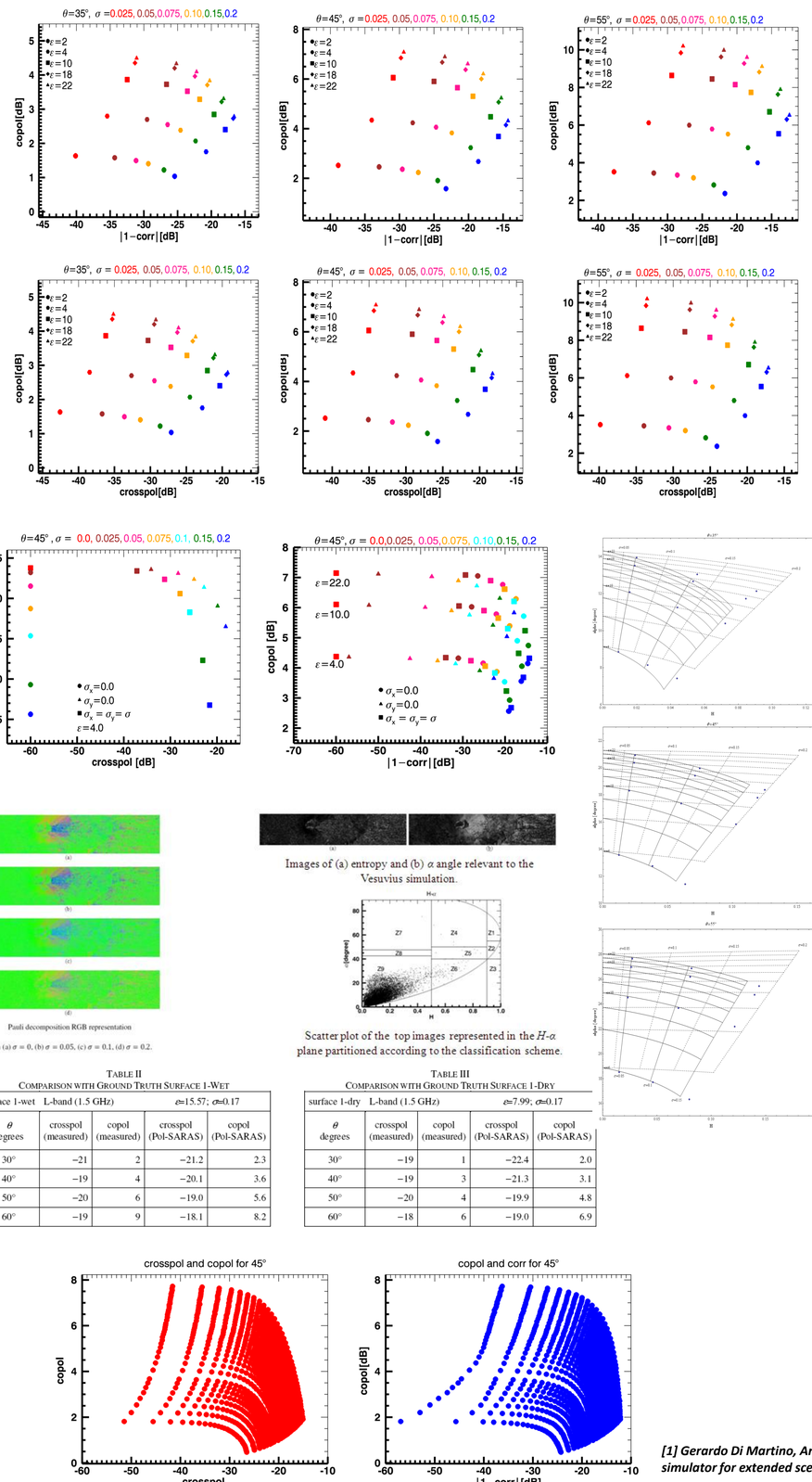

Pauli decomposition RGB representation

with (a) $\sigma = 0$, (b) $\sigma = 0.05$, (c) $\sigma = 0.1$, (d) $\sigma = 0.2$.

Images of (a) entropy and (b) α angle relevant to the Vesuvius simulation.

Scatter plot of the top images represented in the H-α plane partitioned according to the classification scheme.

TABLE II
COMPARISON WITH GROUND TRUTH SURFACE 1-WET

surface 1-wet L-band (1.5 GHz)			ε≈15.57; σ≈0.17	
θ degrees	crosspol (measured)	copol (measured)	crosspol (Pol-SARAS)	copol (Pol-SARAS)
30°	−21	2	−21.2	2.3
40°	−19	4	−20.1	3.6
50°	−20	6	−19.0	5.6
60°	−19	9	−18.1	8.2

TABLE III
COMPARISON WITH GROUND TRUTH SURFACE 1-DRY

surface 1-dry L-band (1.5 GHz)			ε≈7.99; σ≈0.17	
θ degrees	crosspol (measured)	copol (measured)	crosspol (Pol-SARAS)	copol (Pol-SARAS)
30°	−19	1	−22.4	2.0
40°	−19	3	−21.3	3.1
50°	−20	4	−19.9	4.8
60°	−18	6	−19.0	6.9

SAR Interferometry

$$\varphi_{ij}^k = -2\pi a_{ij}^k - \frac{4\pi}{\lambda}\cdot\frac{B_i^\perp}{R_i^m sin\theta_i^m}H_{ij} - \frac{4\pi}{\lambda}D_{ij} + \frac{4\pi}{\lambda}\cdot\frac{B_i^\perp}{R_i^m tan\theta_i^m}\eta_{ij}^m + \frac{2\pi}{v}(f_{dc,i}^m - f_{dc,i}^s)\xi_{ij}^m + f_{\varphi_{orbit}}(\xi_{ij}^m - \eta_{ij}^m) + \varphi_{ijatmo}^k + n_{ij}^k, \quad (2.8)$$

where:

φ_{ij}^k	double-difference phase observation,
$B_i^\perp$, R_i^m,θ_i^m	perpendicular baseline, range and incidence angle for PS i,
a_{ij}^k	integer ambiguity between PS i and PS j,
H_{ij}^k	(residual) topographic height between PS i and PS j,
D_{ij}^k	deformation between PS i and PS j,
ξ_{ij}^m	sub-pixel position in azimuth direction,
η_{ij}^m	slant-range sub-pixel position,
η, ξ	range and azimuth radar coordinates,
v	satellite velocity,
$f_{dc,i}^m$, $f_{dc,i}^s$	Doppler centroid frequency of master and slave acquisition,
$f_{\varphi orbit}(\xi_{ij}^m - \eta_{ij}^m)$	(residual) orbital trend as a function of radar coordinates,
φ_{ijatmo}^k	(residual) atmospheric signal,
n_{ij}^k	measurement noise.

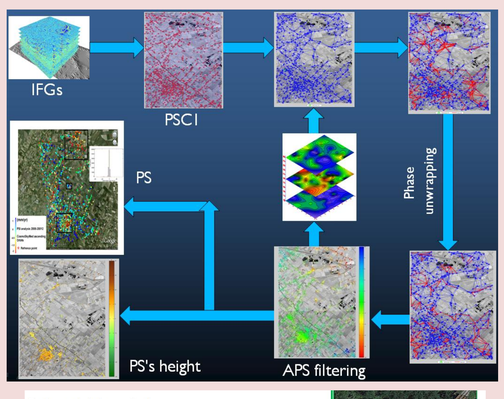

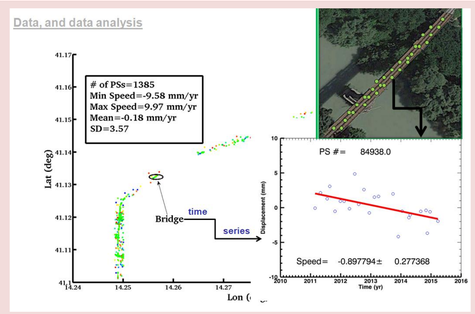

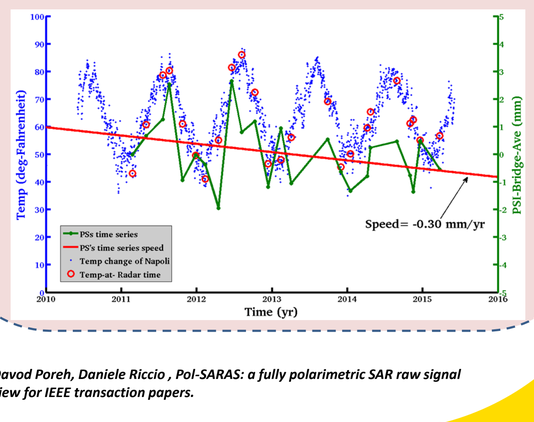

[1] Gerardo Di Martino, Antonio Iodice, Davod Poreh, Daniele Riccio , Pol-SARAS: a fully polarimetric SAR raw signal simulator for extended scenes, Under review for IEEE transaction papers.

CO-OPERATION:

ESA-ASI: for Cosmo-SkyMed (CSK) data.

Future works

- Azimuth correction simulation with Pol-SARAS.
- Look up table generation of Pol-SARAS for different look angles of 20-60°, and comparision with measured data and PTSM methodology.
- PSI analyis for railways monitoring in Campania.